Steel and Composite Structures, *Vol. 29, No. 6 (2018) 755-766*
DOI: https://doi.org/10.12989/scs.2018.29.6.755

Numerical approaches for vibration response of annular and circular composite plates

Ali Kemal Baltacıoğlu and Ömer Civalek*

Akdeniz University, Engineering Faculty, Civil Engineering Department, Division of Mechanics, 07058, Antalya-Turkey

(*Received September 22, 2018, Revised December 10, 2018, Accepted December 11, 2018*)

Abstract. In the present investigation, by using the two numerical methods, free vibration analysis of laminated annular and annular sector plates have been studied. In order to obtain the main equations two different shell theories such as Love's shell theory and first-order shear deformation theory (FSDT) have been used for modeling. After obtaining the fundamental equations in briefly, the methods of harmonic differential quadrature (HDQ) and discrete singular convolution (DSC) are used to solve the equation of motion. Accuracy, convergence and reliability of the present HDQ and DSC methods were tested by comparing the existing results obtained by different methods in the literature. The effects of some geometric and material properties of the plates are investigated via these two methods. The advantages and accuracy of the HDQ and DSC methods have also been examined with different grid numbers and shell theory. Some results for laminated annular plates and laminated circular plates were also been supplied.

Keywords: laminated composites; annular plate; circular plate; differential quadrature; discrete singular convolution

1. Introduction

Plates with curved edges, panels and shells are extensively used in many important engineering applications such as aerospace, marine, civil, mechanical, liquid or gas storage tanks and pipeline, ship hulls, pressure vessels and automobile engineering. In general, laminated composite materials are used for their design Reddy (2003). The main reason for their use is that of high strength to weight ratio. Different plates and shell theories have been proposed and used for modeling of plates and shells for the past hundred years Qatu (2004); Soedel (2004); Reddy (2003); Civalek (2004). After obtaining the reasonable model, the next job is the solution of obtaining differential equations. For this, some numerical and analytical methods are purposed and extensively used by researcher for solution of the resulting equations Leissa (1993); Tornabene *et al*. (2014); Civalek (1988). It is also known that these types of structures are generally subjected to different kind dynamic loads. So, vibration behavior of these structures or their components is very important during their design steps. Up to date, free vibration analysis of annular, circular and sector plates with different material properties has received great attention by the researchers and design engineers. Su *et al*. (2014, 2015) was applied numerical technique for vibration analysis of laminated sector and annular plates. Stability and vibration analysis of composite sector plates have been made by Sharma *et al*. (2005). Three-dimensional frequency response of thick laminated annular sector plates has been investigated by Malekzadeh (2009) via differential quadrature method. Tornabene *et al*. (2013, 2014, 2016) give detailed formulation and solution of curved plates and shells. Strong form FEM formulation for plates has also been derived by Fantuzzi and Tornabene (2014). Civalek (2006a, b, 2013, 2017) gives DSC solution for vibration problems of shells and plates. Detailed unified formulation and solution for plates and shells have given by Wang *et al*. (2016a, b). Free vibration of functionally graded moderately thick annular sector plates have been made by Saidi *et al*. (2011). Kahare and Mittal (2016, 2017) present some solution of circular and annular plates via FEM. Arefi *et al*. (2018) have been supply numerical solution for CNTR cylindrical pressure under thermals effect. Effect of thermal gradients on stress/strain distributions in a thin circular symmetric plate was analzed by Aleksandrova (2016). Hyperbolic shear deformation theory for bending, buckling and free vibration of FGM sandwich plates were made by Abdelaziz *et al*. (2017). Hamzehkolaei *et al*. (2011) present numerical solution for thermal effect on axisymmetric bending of functionally graded circular and annular plates using DQM. Thermal stresses and deflections of functionally graded sandwich plates using a new refined hyperbolic shear deformation theory have been investigated by Bouchafa *et al*. (2015). Bouderba *et al*. (2016) analyzed the thermal stability of functionally graded sandwich plates using a simple shear deformation theory. Thai and Kim (2018) also gives detailed solution for functionally graded plates via new quasi-3D sinusoidal shear deformation theory. Natural vibration characteristics of a clamped circular plate in contact with fluid have been solved by Jhung *et al*. (2005). Tahouneh (2014) present some numerical solution for free vibration analysis of bidirectional functionally graded

*Corresponding author, Ph.D.,
E-mail: civalek@yahoo.com

http://www.techno-press.org/?journal=scs&subpage=6
ISSN: 1229-9367 (Print), 1598-6233 (Online)

annular plates resting on elastic foundations. Yousefzadeh *et al*. (2018) made dynamic response of functionally graded annular/circular plate in contact with bounded fluid under harmonic load. Quasi-3D static analysis of two-directional functionally graded circular plates was solved by Wu and Yu (2018). Also, state space meshless method for the 3D analysis of FGM axisymmetric circular plates have been detailed investigated by Wu and Yu (2016).

The main objective of this manuscript is to obtain the numerical solution for vibration problem of thick laminated annular, annular sector and laminated circular plates based on the two different shells theories. For achieve this, differential quadrature and discrete singular convolution methods are applied to numerically solve the equations of motion for free vibration problem of laminated annular and circular plates. For achieve this, governing equations of motion of annular and annular sector plates are directly obtained via conical shell equations. To solve the governing partial differential equations of motion for plate vibration, two novels numerical methods have been performed and their performance are compared. It is shown that both methods have good convergence. Also, the method of DSC has shown a relatively fast approach with less grid points. Effects of different material and geometric parameters on frequency values of annular and annular sector plates have been investigated.

2. Numerical methods

2.1 Differential quadrature (DQ) method

In differential quadrature procedure, the given differential equation transform into a set of analogous algebraic equations in terms of the unknown function values at the reselected sampling grids in the field domain

$$\left.\frac{\partial^r u}{\partial x^r}\right|_{x=x_i} = \sum_{k=1}^{N_x} A_{ik}^{(r)}\, u(x_k, y_j); \qquad r = 1,2,\ldots\ldots, N_x - 1 \quad (1)$$

$$\left.\frac{\partial^s u}{\partial y^s}\right|_{y=y_j} = \sum_{k=1}^{N_x} B_{jk}^{(s)}\, u(x_i, y_k); \qquad s = 1,2,\ldots\ldots, N_y - 1 \quad (2)$$

$$\left.\frac{\partial^{(r+s)} u}{\partial x^r \partial y^s}\right|_{x_i y_j} = \frac{\partial^r}{\partial x^r}\left(\frac{\partial^s u}{\partial y^s}\right)_{x_i y_j} = \sum_{k=1}^{N_x} A_{ik}^{(r)} \cdot \sum_{m=1}^{N_y} B_{jm}^{(s)} u(x_k, y_m) \quad (3)$$

After the first-order derivation is obtained the second, third and fourth-order derivatives can be easily found as

$$B_{ij} = \sum_{k=1}^{N} A_{ik} A_{kj}, \qquad C_{ij} = \sum_{k=1}^{N} A_{ik} B_{kj}, \qquad D_{ij} = \sum_{k=1}^{N} A_{ik} C_{kj} \quad (4)$$

2.2 Discrete Singular Convolution (DSC) method

Discrete singular convolution (DSC) is suggested by Wei (2001a, b) for the first time in order to fast solution of the mathematical physics problems (Wang *et al*. 2012, Gürses *et al*. 2012, Civalek and Acar 2007, Demir *et al*. 2016, Civalek *et al*. 2016, 2010, Hou *et al*. 2005). As similar the other discrete numerical methods, the function $f(x)$ and its derivatives with respect to the x coordinate at a grid point x_i are approximated by a linear sum of discrete values $f(x_k)$ in a narrow bandwidth $[x-x_M, x+x_M]$ in DSC. Namely

$$\left.\frac{d^n f(x)}{d x^n}\right|_{x=x_i} = f^{(n)}(x) \approx \sum_{k=-M}^{M} \delta_{\Delta,\sigma}^{(n)}(x_i - x_k) f(x_k) \quad (5)$$

In this paper, detailed formulation and mathematical details of the DQ and DSC method are not given; interested readers may refer to the works of (Wei *et al*. 2001, 2002, Gürses *et al*. 2009, Baltacıoğlu *et al*. 2010, 2011, Civalek 2008, 2013, Duan *et al*. 2014, Civalek and Akgöz 2011, Mercan and Civalek 2016). It is mentioned that, the use of the regularized Shannon kernel (RSK) and Lagrange's delta sequence kernel are very effective. These kernels are as follows

$$\delta_{\Delta,\sigma}(x - x_k) = \frac{\sin[(\pi/\Delta)(x - x_k)]}{(\pi/\Delta)(x - x_k)} \exp\left[-\frac{(x - x_k)^2}{2\sigma^2}\right] \quad (6)$$

$$\Re_{i,j}(x) = \begin{cases} \prod_{k=i-M,\, k \neq i+j}^{i+M} \dfrac{x - x_k}{x_{i+j} - x_k}, & x_{i-M} \le x \le x_{i+M}, \\ 0 & \text{otherwise.} \end{cases} \quad (7)$$

The solution also made by harmonic differential quadrature methods (Striz et al. 1995; Shu and Xue 1997; Civalek 2004).

3. Theoretical formulation

Consider a thick laminated annular plates and circular plates.

The circular cylindrical panel is obtained via this figure using the $\alpha = 0$. Also, when we take the $\alpha = 90$ for semi-vertex angle, the new form will be annular sector plate. The

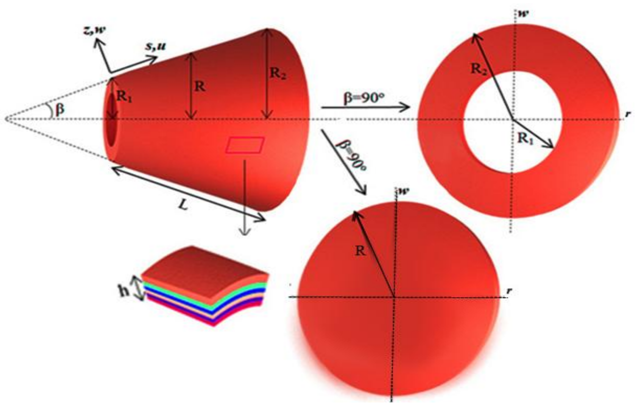

Fig. 1 Geometry and notation of plates from the conical shells

geometry and coordinate axes of these panels and plates is depicted in this figure. The cone semi vertex angle, thickness of the shell, and cone length are denoted by α, h and L, respectively. The shell is referred to a coordinate system (x,s,z). R_1 and R_2 are the by u, v, w in the x, s and z directions, respectively.

3.1 First-order shear deformation theory

The governing differential equations of motion via FSDT

$$\begin{aligned}
&A_{11}\frac{\partial^2 u}{\partial x^2}+\frac{A_{11}}{R(x)}\sin\alpha\frac{\partial u}{\partial x}-\frac{A_{22}}{R^2(x)}\sin^2\alpha\cdot u+\frac{A_{33}}{R^2(x)}\frac{\partial^2 u}{\partial s^2}+\frac{(A_{12}+A_{33})}{R(x)}\frac{\partial^2 v}{\partial x\partial s}\\
&-\frac{(A_{22}+A_{33})}{R^2(x)}\sin\alpha\frac{\partial v}{\partial s}+\frac{A_{12}}{R(x)}\cos\alpha\frac{\partial w}{\partial x}-\frac{A_{22}}{R^2(x)}\sin\alpha\cdot\cos\alpha\cdot w-B_{11}\frac{\partial^2\varphi_x}{\partial x^2}\\
&+\frac{B_{11}}{R(x)}\sin\alpha\frac{\partial\varphi_x}{\partial x}-\frac{B_{22}}{R^2(x)}\sin^2\alpha\cdot\varphi_x+\frac{B_{33}}{R^2(x)}\frac{\partial^2\varphi_x}{\partial s^2}\\
&+\frac{(B_{12}+B_{33})}{R(x)}\frac{\partial^2\varphi_s}{\partial x\partial s}-\frac{(B_{22}+B_{33})}{R^2(x)}\frac{\partial\varphi_s}{\partial s}\sin\alpha=\rho h\frac{\partial^2 u}{\partial t^2}
\end{aligned}\tag{8}$$

$$\begin{aligned}
&\frac{(A_{12}+A_{33})}{R(x)}\frac{\partial^2 u}{\partial x\partial s}+\frac{(A_{22}+A_{33})}{R^2(x)}\sin\alpha\frac{\partial u}{\partial s}+A_{33}\frac{\partial^2 v}{\partial x^2}+A_{33}\frac{\sin\alpha}{R(x)}\frac{\partial v}{\partial x}\\
&-\frac{A_{33}}{R^2(x)}\sin^2\alpha\cdot v+\frac{A_{22}}{R^2(x)}\frac{\partial^2 v}{\partial s^2}-\frac{A_{44}}{R^2(x)}\cos^2\alpha\cdot v+\frac{(A_{22}+A_{44})}{R^2(x)}\cos\alpha\frac{\partial w}{\partial s}\\
&+\frac{(B_{12}+B_{33})}{R(x)}\frac{\partial^2\varphi_x}{\partial x\partial s}+\frac{(B_{22}+B_{33})}{R^2(x)}\sin\alpha\frac{\partial\varphi_x}{\partial s}+B_{33}\frac{\partial^2\varphi_s}{\partial x^2}+B_{33}\frac{\sin\alpha}{R(x)}\frac{\partial\varphi_s}{\partial x}\\
&-\frac{B_{33}}{R^2(x)}\sin^2\alpha\cdot\varphi_s+\frac{B_{22}}{R^2(x)}\frac{\partial^2\varphi_s}{\partial s^2}+A_{44}\frac{\cos\alpha}{R(x)}\cdot\varphi_s=\rho h\frac{\partial^2 v}{\partial t^2}
\end{aligned}\tag{9}$$

$$\begin{aligned}
&-\frac{A_{12}}{R(x)}\cos\alpha\frac{\partial u}{\partial x}-\frac{A_{22}}{R^2(x)}\cdot u\cdot\sin\alpha\cdot\cos\alpha-\frac{(A_{22}+A_{44})}{R^2(x)}\cdot\cos\alpha\frac{\partial v}{\partial s}+A_{55}\frac{\partial^2 w}{\partial x^2}\\
&+\frac{A_{55}}{R(x)}\sin\alpha\cdot\frac{\partial w}{\partial s}+\frac{A_{44}}{R^2(x)}\frac{\partial^2 w}{\partial s^2}-\frac{A_{22}}{R^2(x)}\cdot w\cdot\cos^2\alpha+A_{55}\frac{\partial\varphi_x}{\partial x}-\frac{B_{12}}{R(x)}\cos\alpha\cdot\frac{\partial\varphi_x}{\partial x}\\
&+\frac{A_{55}}{R(x)}\sin\alpha\cdot\varphi_x-\frac{B_{22}}{R^2(x)}\sin\alpha\cdot\cos\alpha\cdot\varphi_x+\frac{A_{44}}{R(x)}\cdot\frac{\partial\varphi_s}{\partial s}\\
&-\frac{B_{22}}{R^2(x)}\cdot\cos\alpha\frac{\partial\varphi_s}{\partial s}=\rho h\frac{\partial^2 w}{\partial t^2}
\end{aligned}\tag{10}$$

$$\begin{aligned}
&B_{11}\frac{\partial^2 u}{\partial x^2}+\frac{B_{11}}{R(x)}\sin\alpha\frac{\partial u}{\partial x}-\frac{B_{22}}{R^2(x)}\cdot u\cdot\sin^2\alpha+\frac{B_{33}}{R^2(x)}\frac{\partial^2 u}{\partial s^2}+\frac{(B_{12}+B_{33})}{R(x)}\frac{\partial^2 v}{\partial x\partial s}\\
&-\frac{(B_{22}+B_{33})}{R^2(x)}\sin\alpha\frac{\partial v}{\partial s}-A_{55}\frac{\partial w}{\partial x}+B_{12}\frac{\cos\alpha}{R(x)}\frac{\partial w}{\partial x}-\frac{B_{22}}{R^2(x)}\cdot w\cdot\sin\alpha\cos\alpha\\
&+D_{11}\frac{\partial^2\varphi_x}{\partial x^2}+D_{11}\frac{\sin\alpha}{R(x)}\frac{\partial\varphi_x}{\partial x}-\frac{D_{22}}{R^2(x)}\varphi_x\sin^2\alpha+\frac{D_{33}}{R^2(x)}\frac{\partial^2\varphi_x}{\partial s^2}-A_{55}\varphi_x\\
&+\frac{(D_{12}+D_{33})}{R(x)}\frac{\partial^2\varphi_s}{\partial x\partial s}-\frac{(D_{22}+D_{33})}{R^2(x)}\frac{\partial\varphi_s}{\partial s}\sin\alpha=\rho h\frac{\partial^2\varphi_x}{\partial t^2}
\end{aligned}\tag{11}$$

$$\begin{aligned}
&\frac{(B_{12}+B_{33})}{R(x)}\frac{\partial^2 u}{\partial x\partial s}+\frac{(B_{22}+B_{33})}{R^2(x)}\frac{\partial u}{\partial s}\sin\alpha+B_{33}\frac{\partial^2 v}{\partial x^2}+B_{33}\frac{\sin\alpha}{R(x)}\frac{\partial v}{\partial x}\\
&-B_{33}\frac{\sin^2\alpha}{R^2(x)}\cdot v+\frac{B_{22}}{R^2(x)}\frac{\partial^2 v}{\partial s^2}+\frac{A_{44}}{R(x)}\cdot v\cdot\cos\alpha-\frac{A_{44}}{R(x)}\frac{\partial w}{\partial s}+\frac{B_{22}}{R^2(x)}\cos\alpha\frac{\partial w}{\partial s}\\
&+\frac{(D_{12}+D_{33})}{R(x)}\frac{\partial^2\varphi_x}{\partial x\partial s}+\frac{(D_{22}+D_{33})}{R^2(x)}\sin\alpha\frac{\partial\varphi_x}{\partial s}-D_{33}\frac{\partial^2\varphi_s}{\partial x^2}\\
&+D_{33}\frac{\sin\alpha}{R(x)}\frac{\partial\varphi_s}{\partial x}-\frac{D_{33}}{R^2(x)}\sin^2\alpha\cdot\varphi_s+\frac{D_{22}}{R^2(x)}\frac{\partial^2\varphi_s}{\partial s^2}-A_{44}\cdot\varphi_s=\rho h\frac{\partial^2\varphi_s}{\partial t^2}
\end{aligned}\tag{12}$$

We assume the harmonic functions fort the displacement of the conical shell as

$$\begin{Bmatrix} u(x,s,t)\\ v(x,s,t)\\ w(x,s,t)\\ \varphi_x(x,s,t)\\ \varphi_s(x,s,t)\end{Bmatrix}=e^{i\omega t}\begin{Bmatrix} U(x,s,t)\\ V(x,s,t)\\ W(x,s,t)\\ \Psi_x(x,s,t)\\ \Psi_s(x,s,t))\end{Bmatrix}\tag{13}$$

After using Eqs. (13) in Eqs. (8)-(12) related equations can be written in suitable form as

$$L_{11}+L_{12}+L_{13}+L_{14}+L_{15}-\rho h\cdot\omega^2=0\tag{14a}$$

$$L_{21}+L_{22}+L_{23}+L_{24}+L_{25}-\rho h\cdot\omega^2=0\tag{14b}$$

$$L_{31}\cdot U+L_{32}\cdot V+L_{33}\cdot W+L_{34}\cdot\Phi_x+L_{35}\cdot\Phi_y-\rho h\cdot\omega^2=0\tag{14c}$$

$$L_{41}\cdot U+L_{42}\cdot V+L_{43}\cdot W+L_{44}\cdot\Phi_x+L_{45}\cdot\Phi_y-\rho h^3\cdot\omega^2/12=0\tag{14d}$$

$$L_{51}\cdot U+L_{52}\cdot V+L_{53}\cdot W+L_{54}\cdot\Phi_x+L_{55}\cdot\Phi_y-\rho h^3\cdot\omega^2/12=0\tag{14e}$$

Differential operators in Eq. (14) are listed in appendix A.

3.2 Love's shell theory

Equations of motions are written as below in this theory

$$\begin{aligned}
&A_{11}\frac{\partial^2 u}{\partial x^2}+\frac{A_{11}}{R(x)}\sin\alpha\frac{\partial u}{\partial x}-\frac{A_{22}}{R^2(x)}\sin^2\alpha\cdot u+\frac{A_{66}}{R^2(x)}\frac{\partial^2 u}{\partial s^2}\\
&-\frac{(A_{22}+A_{66})}{R^2(x)}\sin\alpha\frac{\partial v}{\partial s}+\frac{(A_{12}+A_{66})}{R(x)}\frac{\partial^2 v}{\partial x\partial s}\\
&+\frac{(B_{12}+2B_{66})}{R^2(x)}\frac{\partial^2 v}{\partial x\partial s}-\frac{(B_{12}+B_{22}+2B_{66})}{R^2(x)}\frac{\partial v}{\partial s}\\
&+\frac{A_{12}}{R(x)}\cos\alpha\frac{\partial w}{\partial x}-\frac{A_{22}}{R^2(x)}\sin\alpha\cdot\cos\alpha\cdot w-B_{11}\cdot\frac{\partial w}{\partial s}-\frac{(B_{12}+2\cdot B_{66})}{R^2(x)}\frac{\partial^3 w}{\partial x\partial s^2}\\
&-\frac{B_{11}}{R(x)}\sin\alpha\frac{\partial^2 w}{\partial x^2}+\frac{(B_{12}+B_{22}+2\cdot B_{66})}{R^3(x)}\sin\alpha\frac{\partial^2 w}{\partial s^2}+\frac{B_{22}}{R^2(x)}\sin^2\alpha\frac{\partial w}{\partial x}=\rho h\frac{\partial^2 u}{\partial t^2}
\end{aligned}\tag{15}$$

$$\begin{aligned}
&\frac{(A_{12}+A_{66})}{R(x)}\frac{\partial^2 u}{\partial x\partial s}+\frac{(A_{22}+A_{66})}{R^2(x)}\sin\alpha\frac{\partial u}{\partial s}+\frac{(B_{12}+B_{66})\cos\alpha}{R^2(x)}\frac{\partial^2 u}{\partial x\partial s}\\
&+\frac{(B_{22}-B_{66})\sin\alpha\cos\alpha}{R^3(x)}\frac{\partial u}{\partial s}\\
&-\frac{A_{66}}{R^2(x)}\sin^2\alpha\cdot v+A_{66}\frac{\partial^2 v}{\partial s^2}+\frac{A_{66}}{R(x)}\sin\alpha\frac{\partial v}{\partial x}+\frac{A_{22}}{R^2(x)}\frac{\partial^2 v}{\partial s^2}+2\frac{B_{22}}{R^3(x)}\cos\alpha\frac{\partial^2 v}{\partial s^2}\\
&+\frac{D_{22}}{R^4(x)}\cos^2\alpha\cdot\frac{\partial^2 v}{\partial s^2}+\frac{3B_{66}}{R(x)}\cos\alpha\frac{\partial^2 v}{\partial s^2}-\frac{1}{R(x)}\sin\alpha\frac{\partial v}{\partial x}+\frac{B_{66}}{R^3(x)}\cos\alpha\cdot\sin^2\alpha\\
&+2\frac{D_{66}}{R^2(x)}\cos^2\alpha\frac{\partial^2 v}{\partial x^2}-4\frac{D_{66}}{R^3(x)}\cos^2\alpha\cdot\sin\alpha\frac{\partial v}{\partial x}\\
&+4\frac{D_{66}}{R^4(x)}\cos^2\alpha\cdot\sin^2\alpha\cdot v+\frac{A_{22}}{R^2(x)}\cos\alpha\frac{\partial w}{\partial s}+\frac{B_{22}}{R^3(x)}\cos^2\alpha\frac{\partial w}{\partial s}\\
&-4\frac{D_{66}\sin^2\alpha\cos\alpha}{R^4(x)}\frac{\partial w}{\partial s}-\frac{B_{22}}{R^3(x)}\frac{\partial^3 w}{\partial s^3}-\frac{D_{22}}{R^4(x)}\cos\alpha\frac{\partial^3 w}{\partial s^3}\\
&-\frac{B_{22}\sin\alpha}{R^2(x)}\frac{\partial^2 w}{\partial x\partial s}+\frac{D_{22}}{R^3(x)}\sin\alpha\cos\alpha\frac{\partial^2 w}{\partial x\partial s}-\frac{4D_{66}}{R^3(x)}\sin\alpha\cos\alpha\frac{\partial^2 w}{\partial x\partial s}\\
&-\frac{(D_{12}+2D_{66})\cos\alpha}{R^2(x)}\frac{\partial^3 w}{\partial x^2\partial s}+\frac{(B_{12}+2B_{66})\cos\alpha}{R(x)}\frac{\partial^3 w}{\partial x^2\partial s}=\rho h\frac{\partial^2 v}{\partial t^2}
\end{aligned}\tag{16}$$

$$-\frac{A_{12}}{R(x)}\cos\alpha\frac{\partial u}{\partial x}-\frac{A_{22}}{R^2(x)}\cdot u\cdot\sin\alpha\cdot\cos\alpha+B_{11}\frac{\partial^3 u}{\partial x^3}+\frac{(B_{12}+2B_{66})}{R^2(x}\frac{\partial^3 u}{\partial x\partial s^2}\tag{17}$$

$$
\begin{aligned}
&+2\frac{B_{11}}{R(x)}\sin\alpha\frac{\partial^2 u}{\partial x^2}-\frac{B_{22}}{R^2(x)}\cdot\sin^2\alpha\frac{\partial u}{\partial x}\cdot+\frac{B_{22}}{R^3(x)}\cdot\sin^3\alpha\cdot u+\frac{(B_{22}-2B_{66})}{R^3(x}\frac{\partial^2 u}{\partial s^2}\\
&-\frac{A_{22}}{R(x)}\cos\alpha\frac{\partial v}{\partial s}-\frac{B_{22}}{R^3(x)}\cdot\cos^2\alpha\frac{\partial v}{\partial s}\cdot+\frac{(B_{22}+2B_{66})}{R^3(x)}\sin^2\alpha\frac{\partial v}{\partial s}\\
&+\frac{(2D_{12}+2D_{22}+8D_{66})}{R^4(x)}\cos\alpha\sin^2\alpha\frac{\partial v}{\partial s}+\left(\frac{B_{22}}{R^3(x)}+\frac{D_{22}\cos\alpha}{R^4(x)}\right)\frac{\partial^3 v}{\partial s^3}\\
&+R(x)\left(\frac{B_{12}+2B_{66}}{R^2(x)}+\frac{(D_{12}+4D_{66})\cos\alpha}{R^3(x)}\right)\frac{\partial^3 v}{\partial x^2\partial s}\\
&+\frac{(D_{22}+2D_{12}+8D_{66})}{R^3(x)}\cos\alpha\sin\alpha\cdot\frac{\partial^2 v}{\partial x\partial s}-\left(\frac{B_{22}+2B_{66}}{R^2(x)}\sin\alpha\right)\frac{\partial^2 v}{\partial x\partial s}\\
&-\frac{A_{22}}{R^2(x)}\cos^2\alpha\cdot w+2B_{12}\frac{1}{R(x)}\frac{\partial^2 w}{\partial x^2}+2\frac{B_{22}}{R^3(x)}\cos\alpha\cdot\frac{\partial^2 w}{\partial s^2}+\frac{B_{22}}{R^3(x)}\cos\alpha\cdot\sin^2\alpha\cdot w\\
&-D_{11}\frac{\partial^4 w}{\partial x^4}-\frac{2D_{12}+4D_{66}}{R^2(x)}\frac{\partial^4 w}{\partial x^2\partial s^2}-\frac{D_{22}}{R^4(x)}\frac{\partial^4 w}{\partial s^4}\\
&-\frac{2D_{11}}{R(x)}\sin\alpha\frac{\partial^3 w}{\partial s^3}+\frac{2D_{12}+8D_{66}}{R^3(x)}\sin\alpha\frac{\partial^3 w}{\partial x\partial s^2}+\frac{D_{22}}{R^2(x)}\sin^2\alpha\frac{\partial^2 w}{\partial x^2}\\
&-\frac{(2D_{12}+2D_{22}+8D_{66})}{R^4(x)}\sin^2\alpha\frac{\partial^2 w}{\partial s^2}-\frac{D_{22}}{R^3(x)}\sin^3\alpha\frac{\partial w}{\partial x}=\rho h\frac{\partial^2 w}{\partial t^2}
\end{aligned}
\tag{17}
$$

If the displacement terms are taken as below

$$u=U(x)\cdot\cos(ns)\cdot\cos(\omega t),\tag{18a}$$

$$v=V(x)\cdot\sin(ns)\cdot\cos(\omega t),\tag{18b}$$

$$w=W(x)\cdot\cos(ns)\cdot\cos(\omega t).\tag{18c}$$

Substituting Eq. (18) into Eqs. (15)-(17), we eliminate the s and t and the governing equations of motions for conical panel based on Love's shell theory can be written as

$$
\begin{aligned}
&G_{111}U+G_{112}\frac{\partial U}{\partial x}+G_{113}\frac{\partial^2 U}{\partial x^2}+G_{121}V+G_{122}\frac{\partial V}{\partial x}+G_{131}W+G_{132}\frac{\partial W}{\partial x}\\
&+G_{133}\frac{\partial^2 W}{\partial x^2}+G_{134}\frac{\partial^3 W}{\partial x^3}=-\rho h\omega^2 U
\end{aligned}
\tag{19}
$$

$$
\begin{aligned}
&G_{211}U+G_{212}\frac{\partial U}{\partial x}+G_{221}V+G_{222}\frac{\partial V}{\partial x}+G_{223}\frac{\partial^2 V}{\partial x^2}\\
&+G_{231}W+G_{232}\frac{\partial W}{\partial x}=-\rho h\omega^2 V
\end{aligned}
\tag{20}
$$

$$
\begin{aligned}
&G_{311}U+G_{312}\frac{\partial U}{\partial x}+G_{313}\frac{\partial^2 U}{\partial x^2}+G_{314}\frac{\partial^3 U}{\partial x^3}+G_{321}V+G_{322}\frac{\partial V}{\partial x}+G_{323}\frac{\partial^2 V}{\partial x^2}\\
&+G_{331}W+G_{332}\frac{\partial W}{\partial x}+G_{333}\frac{\partial^2 W}{\partial x^2}+G_{334}\frac{\partial^3 W}{\partial x^3}+G_{335}\frac{\partial^4 W}{\partial x^4}=-\rho h\omega^2 W
\end{aligned}
\tag{21}
$$

where G_{ijk} are the constant coefficients defined in Appendix B.

4. Solution via numerical methods

4.1 Solution by DSC method based on FSDT theory

After applying the DSC method, the related equations of motion of laminated annular plate were discrete and given as

$$
\begin{aligned}
&{}^{DSC}L_{11}\cdot U+{}^{DSC}L_{12}\cdot V+{}^{DSC}L_{13}\cdot W+{}^{DSC}L_{14}\cdot\Phi_x+{}^{DSC}L_{15}\cdot\Phi_y-\rho h\cdot\omega^2=0\\
&{}^{DSC}L_{21}\cdot U+{}^{DSC}L_{22}\cdot V+{}^{DSC}L_{23}\cdot W+{}^{DSC}L_{24}\cdot\Phi_x+{}^{DSC}L_{25}\cdot\Phi_y-\rho h\cdot\omega^2=0\\
&{}^{DSC}L_{31}\cdot U+{}^{DSC}L_{32}\cdot V+{}^{DSC}L_{33}\cdot W+{}^{DSC}L_{34}\cdot\Phi_x+{}^{DSC}L_{35}\cdot\Phi_y-\rho h\cdot\omega^2=0\\
&{}^{DSC}L_{41}\cdot U+{}^{DSC}L_{42}\cdot V+{}^{DSC}L_{43}\cdot W+{}^{DSC}L_{44}\cdot\Phi_x+{}^{DSC}L_{45}\cdot\Phi_y-\rho h^3\cdot\omega^2/12=0\\
&{}^{DSC}L_{51}\cdot U+{}^{DSC}L_{52}\cdot V+{}^{DSC}L_{53}\cdot W+{}^{DSC}L_{54}\cdot\Phi_x+{}^{DSC}L_{55}\cdot\Phi_y-\rho h^3\cdot\omega^2/12=0
\end{aligned}
\tag{22}
$$

The coefficients of L_{ij} given above equation are obtained after application of DSC rule. Discrete form of the related differential operators can be defined as

$${}^{DSC}L_{11}=A_{11}\cdot\Xi_x^{(2)}+\frac{A_{11}}{R(x)}\sin\alpha\cdot\Xi_x^{(1)}-\frac{A_{22}}{R^2(x)}\cdot U(i)\cdot\sin^2\alpha+\frac{A_{33}}{R^2(x)}\cdot\Xi_s^{(2)}\tag{23}$$

$${}^{DSC}L_{12}=\frac{(A_{12}+A_{33})}{R(x)}\sin\alpha\cdot\Xi_{xs}^{(2)}\frac{\partial^2 V}{\partial x\partial s}-\frac{(A_{22}+A_{33})}{R^2(x)}\sin\alpha\cdot\Xi_s^{(1)}\tag{24}$$

$${}^{DSC}L_{13}=\frac{A_{12}}{R(x)}\cos\alpha\cdot\Xi_x^{(1)}-\frac{A_{22}}{R^2(x)}\cdot W(i)\cdot\sin\alpha\cdot\cos\alpha\tag{25}$$

$${}^{DSC}L_{14}=B_{11}\cdot\Xi_x^{(2)}+\frac{B_{11}}{R(x)}\sin\alpha\cdot\Xi_x^{(1)}-\frac{B_{22}}{R^2(x)}\cdot\Psi_x(i)\sin^2\alpha+\frac{B_{33}}{R^2(x)}\cdot\Xi_s^{(2)}\tag{26}$$

$${}^{DSC}L_{15}=\frac{(B_{12}+B_{33})}{R(x)}\cdot\Xi_x^{(1)}\cdot\Xi_s^{(1)}-\frac{(B_{22}+B_{33})}{R^2(x)}\cdot\Xi_s^{(1)}\cdot\sin\alpha\tag{27}$$

$${}^{DSC}L_{21}=\frac{(A_{12}+A_{33})}{R(x)}\cdot\Xi_x^{(1)}\cdot\Xi_s^{(1)}+\frac{(A_{22}+A_{33})}{R^2(x)}\sin\alpha\cdot\Xi_s^{(1)}\tag{28}$$

$$
\begin{aligned}
&{}^{DSC}L_{22}=A_{33}\Xi_x^{(2)}+A_{33}\frac{\sin\alpha}{R(x)}\Xi_s^{(1)}\\
&-\frac{A_{33}}{R^2(x)}\cdot V(i)\cdot\sin^2\alpha+\frac{A_{22}}{R^2(x)}\Xi_s^{(2)}-\frac{A_{44}}{R^2(x)}\cdot V(i)\cdot\cos^2\alpha
\end{aligned}
\tag{29}
$$

$${}^{DSC}L_{23}=\frac{(A_{22}+A_{44})}{R^2(x)}\cdot\cos\alpha\cdot\Xi_s^{(1)}\tag{30}$$

$${}^{DSC}L_{24}=\frac{(B_{12}+B_{33})}{R(x)}\cdot\Xi_x^{(1)}\cdot\Xi_s^{(1)}+\frac{(B_{22}+B_{33})}{R^2(x)}\sin\alpha\cdot\Xi_s^{(1)}\tag{31}$$

$$
\begin{aligned}
&{}^{DSC}L_{25}=B_{33}\cdot\Xi_x^{(2)}+B_{33}\frac{\sin\alpha}{R(x)}\cdot\Xi_x^{(1)}\\
&-\frac{B_{33}}{R^2(x)}\cdot\Psi_s(i)\cdot\sin^2\alpha+\frac{B_{22}}{R^2(x)}\cdot\Xi_s^{(2)}+A_{44}\cdot\frac{\cos\alpha}{R(x)}\cdot\Psi_s(i)
\end{aligned}
\tag{32}
$$

$${}^{DSC}L_{31}=-\frac{A_{12}}{R(x)}\cos\alpha\cdot\Xi_x^{(1)}-\frac{A_{22}}{R^2(x)}\cdot U(i)\cdot\sin\alpha\cdot\cos\alpha\tag{33}$$

$${}^{DSC}L_{32}=-\frac{(A_{22}+A_{44})}{R^2(x)}\cos\alpha\cdot\Xi_s^{(1)}\tag{34}$$

$${}^{DSC}L_{33}=A_{55}\cdot\Xi_x^{(2)}+\frac{A_{55}}{R(x)}\sin\alpha\cdot\Xi_s^{(1)}+\frac{A_{44}}{R^2(x)}\cdot\Xi_s^{(2)}-\frac{A_{22}}{R^2(x)}\cdot W(i)\cdot\cos^2\alpha\tag{35}$$

$$
\begin{aligned}
&{}^{DSC}L_{34}=A_{55}\cdot\Xi_x^{(1)}-\frac{B_{12}}{R(x)}\cos\alpha\cdot\Xi_x^{(1)}\\
&+\frac{A_{55}}{R(x)}\cdot\Psi_x(i)\cdot\sin\alpha-\frac{B_{22}}{R^2(x)}\cdot\Psi_x(i)\cdot\sin\alpha\cdot\cos\alpha
\end{aligned}
\tag{36}
$$

$${}^{DSC}L_{35}=\frac{A_{44}}{R(x)}\cdot\Xi_s^{(1)}-\frac{B_{22}}{R^2(x)}\cdot\cos\alpha\cdot\Xi_s^{(1)}\tag{37}$$

$$^{DSC}L_{41}=B_{11}\cdot\Xi_x^{(2)}+\frac{B_{11}}{R(x)}\sin\alpha\cdot\Xi_x^{(1)}-\frac{B_{22}}{R^2(x)}\cdot U(i)\cdot\sin^2\alpha+\frac{B_{33}}{R^2(x)}\cdot\Xi_s^{(2)} \quad (38)$$

$$^{DSC}L_{42}=\frac{(B_{12}+B_{33})}{R(x)}\cdot\Xi_x^{(1)}\cdot\Xi_s^{(1)}-\frac{(B_{22}+B_{33})}{R^2(x)}\sin\alpha\cdot\Xi_s^{(1)} \quad (39)$$

$$^{DSC}L_{43}=-A_{55}\cdot\Xi_x^{(1)}+B_{12}\frac{\cos\alpha}{R(x)}\cdot\Xi_x^{(1)}-\frac{B_{22}}{R^2(x)}\cdot W(i)\cdot\sin\alpha\cos\alpha \quad (40)$$

$$^{DSC}L_{44}=D_{11}\cdot\Xi_x^{(2)}+D_{11}\frac{\sin\alpha}{R(x)}\cdot\Xi_x^{(1)}-\frac{D_{22}}{R^2(x)}\sin^2\alpha+\frac{D_{33}}{R^2(x)}\cdot\Xi_s^{(2)}-A_{55}\cdot\Psi_x(i) \quad (41)$$

$$^{DSC}L_{45}=\frac{(D_{12}+D_{33})}{R(x)}\cdot\Xi_x^{(1)}\cdot\Xi_s^{(1)}-\frac{(D_{22}+D_{33})}{R^2(x)}\cdot\Xi_s^{(1)}\sin\alpha \quad (42)$$

$$^{DSC}L_{51}=\frac{(B_{12}+B_{33})}{R(x)}\cdot\Xi_x^{(1)}\cdot\Xi_s^{(1)}+\frac{(B_{22}+B_{33})}{R^2(x)}\cdot\Xi_s^{(1)}\sin\alpha \quad (43)$$

$$\begin{aligned}&^{DSC}L_{52}=B_{33}\cdot\Xi_x^{(2)}+B_{33}\frac{\sin\alpha}{R(x)}\cdot\Xi_x^{(1)}\\&-B_{33}\cdot\frac{\sin^2\alpha}{R^2(x)}\cdot V(i)+\frac{B_{22}}{R^2(x)}\cdot\Xi_s^{(2)}+\frac{A_{44}}{R(x)}\cdot V(i)\cdot\cos\alpha\end{aligned} \quad (44)$$

$$^{DSC}L_{53}=-\frac{A_{44}}{R(x)}\cdot\Xi_s^{(1)}+\frac{B_{22}}{R^2(x)}\cos\alpha\cdot\Xi_s^{(1)} \quad (45)$$

$$^{DSC}L_{54}=\frac{(D_{12}+D_{33})}{R(x)}\cdot\Xi_x^{(1)}\cdot\Xi_s^{(1)}+\frac{(D_{22}+D_{33})}{R^2(x)}\sin\alpha\cdot\Xi_s^{(1)} \quad (46)$$

$$\begin{aligned}&^{DSC}L_{55}=D_{33}\cdot\Xi_x^{(1)}+D_{33}\frac{\sin\alpha}{R(x)}\cdot\Xi_x^{(1)}\\&-\frac{D_{33}}{R^2(x)}\cdot\Psi_s(i)\cdot\sin^2\alpha+\frac{D_{22}}{R^2(x)}\cdot\Xi_s^{(2)}-A_{44}\cdot\Psi_s(i)\end{aligned} \quad (47)$$

The operator of DSC using above can be given by

$$\Xi_x^n(\,)=\frac{\partial^{(n)}(\,)}{\partial x^{(n)}}=\sum_{k=-M}^{M}\delta_{\Delta,\sigma}^{(n)}(k\cdot\Delta x)(\,)_{i+k,j} \quad (48)$$

$$\Xi_s^n(\,)=\frac{\partial^{(n)}(\,)}{\partial s^{(n)}}=\sum_{k=-M}^{M}\delta_{\Delta,\sigma}^{(n)}(k\cdot\Delta s)(\,)_{i,j+k} \quad (49)$$

$$\Xi_x^1\Xi_s^{(n-1)}(\,)=\sum_{k=-M}^{M}\delta_{\Delta,\sigma}^{(1)}(k\cdot\Delta x)(\,)_{i+k,j}\sum_{k=-M}^{M}\delta_{\Delta,\sigma}^{(n-1)}(k\cdot\Delta s)(\,)_{i,k+j} \quad (50)$$

$$\Xi_x^{(n-1)}\Xi_s^1(\,)=\sum_{k=-M}^{M}\delta_{\Delta,\sigma}^{(n-1)}(k\cdot\Delta x)(\,)_{i+k,j}\sum_{k=-M}^{M}\delta_{\Delta,\sigma}^{(1)}(k\cdot\Delta s)(\,)_{i,k+j} \quad (51)$$

4.2 Solution by DQ method based on FSDT

Related coefficients for partial derivations via DQ can be defined by

$$\Xi_x^n(*)=\frac{\partial^{(n)}(*)}{\partial x^{(n)}}=\sum_{k=1}^{N}C_{i+k,j}^{(n)}(i)(*)_{i+k,j} \quad (52)$$

$$\Xi_s^n(*)=\frac{\partial^{(n)}(*)}{\partial s^{(n)}}=\sum_{k=1}^{N}C_{i,j+k}^{(n)}(j)(*)_{i,j+k} \quad (53)$$

$$\Xi_x^1\Xi_s^{(n-1)}(*)=\sum_{k=1}^{N}C_{i+k,j}(i)\sum_{k=1}^{N}C_{i,k+j}^{(n-1)}(j)(*)_{i,k+j} \quad (54)$$

$$\Xi_x^{(n-1)}\Xi_s^1(*)=\frac{\partial^{(n)}(*)}{\partial x^{(n-1)}\partial s}=\sum_{k=1}^{N}C_{i,k+j}^{(n-1)}(j)\sum_{k=1}^{N}C_{i+k,j}^{(1)}(i)(*)_{i,k+j} \quad (55)$$

in which C_{ijk} are weighting coefficients for DQ methods of any order. If the method of DQ is used for discretization, the equation of motion can be writing as follows

$$\begin{aligned}&^{DQ}L_{11}\cdot U+{}^{DQ}L_{12}\cdot V+{}^{DQ}L_{13}\cdot W+{}^{DQ}L_{14}\cdot\Phi_x+{}^{DQ}L_{15}\cdot\Phi_y-\rho h\cdot\omega^2=0\\&^{DQ}L_{21}\cdot U+{}^{DQ}L_{22}\cdot V+{}^{DQ}L_{23}\cdot W+{}^{DQ}L_{24}\cdot\Phi_x+{}^{DQ}L_{25}\cdot\Phi_y-\rho h\cdot\omega^2=0\\&^{DQ}L_{31}\cdot U+{}^{DQ}L_{32}\cdot V+{}^{DQ}L_{33}\cdot W+{}^{DQ}L_{34}\cdot\Phi_x+{}^{DQ}L_{35}\cdot\Phi_y-\rho h\cdot\omega^2=0\\&^{DQ}L_{41}\cdot U+{}^{DQ}L_{42}\cdot V+{}^{DQ}L_{43}\cdot W+{}^{DQ}L_{44}\cdot\Phi_x+{}^{DQ}L_{45}\cdot\Phi_y-\rho h^3\cdot\omega^2/12=0\\&^{DQ}L_{51}\cdot U+{}^{DQ}L_{52}\cdot V+{}^{DQ}L_{53}\cdot W+{}^{DQ}L_{54}\cdot\Phi_x+{}^{DQ}L_{55}\cdot\Phi_y-\rho h^3\cdot\omega^2/12=0\end{aligned} \quad (56)$$

Related derivations for DQ can be written as similar the DSC method.

4.3 Solution by DSC method based on Love's shell theory

The discretized forms of Eq. (56) can then be expressed as

$$\begin{aligned}&G_{111}U_{i,j}+G_{112}\sum_{k=-M}^{M}\delta_{\Delta,\sigma}^{(1)}(k\Delta x)U_{i+k,j}+G_{113}\sum_{k=-M}^{M}\delta_{\Delta,\sigma}^{(2)}(k\Delta x)U_{i+k,j}\\&+G_{121}V_{i,j}+G_{122}\sum_{k=-M}^{M}\delta_{\Delta,\sigma}^{(1)}(k\Delta x)V_{i,j+k}+G_{131}W_{i,j}+G_{1}\\&+G_{122}\sum_{k=-M}^{M}\delta_{\Delta,\sigma}^{(1)}(k\Delta x)V_{i,j+k}+G_{131}W_{i,j}+G_{132}\sum_{k=-M}^{M}\delta_{\Delta,\sigma}^{(1)}(k\Delta x)W_{i,j+k}\\&=-\rho h\omega^2U_{i,j}\end{aligned} \quad (57)$$

$$\begin{aligned}&G_{211}U_{i,j}+G_{212}\sum_{k=-M}^{M}\delta_{\Delta,\sigma}^{(1)}(k\Delta x)U_{i+k,j}+G_{221}V_{i,j}\\&+G_{122}\sum_{k=-M}^{M}\delta_{\Delta,\sigma}^{(1)}(k\Delta x)V_{i,j+k}+G_{223}\sum_{k=-M}^{M}\delta_{\Delta,\sigma}^{(2)}(k\Delta x)V_{i+k,j}\\&+G_{231}W_{i,j}+G_{232}\sum_{k=-M}^{M}\delta_{\Delta,\sigma}^{(1)}(k\Delta x)W_{i,j+k}\\&+G_{233}\sum_{k=-M}^{M}\delta_{\Delta,\sigma}^{(2)}(k\Delta x)W_{i+k,j}=-\rho h\omega^2V_{i,j}\end{aligned} \quad (58)$$

$$\begin{aligned}&G_{311}U_{i,j}+G_{312}\sum_{k=-M}^{M}\delta_{\Delta,\sigma}^{(1)}(k\Delta x)U_{i+k,j}+G_{321}V_{i,j}\\&+G_{322}\sum_{k=-M}^{M}\delta_{\Delta,\sigma}^{(1)}(k\Delta x)V_{i,j+k}+G_{323}\sum_{k=-M}^{M}\delta_{\Delta,\sigma}^{(2)}(k\Delta x)V_{i+k,j}\\&+G_{331}W_{i,j}+G_{332}\sum_{k=-M}^{M}\delta_{\Delta,\sigma}^{(1)}(k\Delta x)W_{i,j+k}+G_{333}\sum_{k=-M}^{M}\delta_{\Delta,\sigma}^{(2)}(k\Delta x)W_{i+k,j}\\&+G_{334}\sum_{k=-M}^{M}\delta_{\Delta,\sigma}^{(3)}(k\Delta x)W_{i+k,j}+G_{335}\sum_{k=-M}^{M}\delta_{\Delta,\sigma}^{(4)}(k\Delta x)W_{i+k,j}\\&=-\rho h\omega^2W_{i,j}\end{aligned} \quad (59)$$

4.4 Solution by DQ method based on Love's shell theory

The discretized forms via DQ method is as follows

$$\begin{aligned}&G_{111}U_k+G_{112}\sum_{k=1}^{N}C_{ik}^{(1)}U_k+G_{113}\sum_{k=1}^{N}C_{ik}^{(2)}U_k+G_{121}V_k\\&+G_{122}\sum_{k=1}^{N}C_{ik}^{(1)}V_k+G_{131}W_k+G_{132}\sum_{k=1}^{N}C_{ik}^{(1)}WV_k=-\rho h\omega^2U_k\end{aligned} \quad (60)$$

$$G_{211}U_k + G_{212}\sum_{k=1}^{N} C_{ik}^{(1)} U_k + G_{221}V_k + G_{122}\sum_{k=1}^{N} C_{ik}^{(1)} V_k + G_{223}\sum_{k=1}^{N} C_{ik}^{(2)} V_k + G_{231}W_k + G_{232}\sum_{k=1}^{N} C_{ik}^{(1)} W_k + G_{233}\sum_{k=1}^{N} C_{ik}^{(2)} W_k = -\rho h \omega^2 V_k \quad (61)$$

$$G_{311}U_k + G_{312}\sum_{k=1}^{N} C_{ik}^{(1)} U_k + G_{321}V_k + G_{322}\sum_{k=1}^{N} C_{ik}^{(1)} V_k + G_{323}\sum_{k=1}^{N} C_{ik}^{(2)} V_k + G_{331}W_{i,j} + G_{332}\sum_{k=1}^{N} C_{ik}^{(1)} W_k + G_{333}\sum_{k=1}^{N} C_{ik}^{(2)} W_k + G_{334}\sum_{k=1}^{N} C_{ik}^{(3)} W_k + G_{335}\sum_{k=1}^{N} C_{ik}^{(4)} W_k = -\rho h \omega^2 W_k \quad (62)$$

For computation three different boundary conditions have been taken into consideration listed below

Simply supported edge (S)

$$V = 0, \quad W = 0, \quad V = 0, \quad M_x = 0, \quad \Psi_s = 0 = 0 \quad (63)$$

Clamped edge (C)

$$U = 0, \quad V = 0, \quad W = 0, \quad \Psi_x = 0, \quad \Psi_s = 0 \quad (64)$$

Free edge (F)

$$V_x = 0, \quad N_x = 0, \quad N_\theta = 0, \quad M_x = 0, \quad \text{and} \quad M_\theta = 0 \quad (65)$$

From the above procedures, one can derive the general form of eigenvalue equation as follows

$$[G]\{X\} = \Omega[B]\{X\} \quad (66)$$

5. Numerical results

In order to validate the presented two numerical methods and to examine their computational efficiency, convergence and accuracy is demonstrated for different plate examples. As a first example to validate the presented formulations, the obtained natural frequencies of a laminated (0/90) annular sector plates with clamped edges based on the presented methods are compared with the FSDT by Pang *et al*. (2007) in Table 1. The results are prepared for different values of modes. From this table, one could observe that the present DSC results for the laminated (0/90) annular sector plates are in good agreement with those of FSDT. Comparison of frequency values of isotropic circular plates with simply supported edges and annular plates have also been made and summarized in Tables 2 and 3. It is again showed that our DSC results are good agreement in literature (Khare and Mittal 2017, Wang *et al*. 2016b). In Table 4, non-dimensional frequencies in five modes of laminated annular sector plates have been listed for different thickness. It can be found that thickness to-radius ratio have a significant influence on the frequency. When the thickness to-radius ratio increased the frequency values decreases. This case also shown in Fig. 2 for laminated annular plates. This ratio is more significant on higher modes.

Some detailed analyses on thickness-to-radii ratio have been also made and given in Tables 5-7 for circular and annular plates. It is concluded from these results that, the sector angles and mode numbers have also important role on this change. Namely, the thickness to-radius ratio is more effective on higher modes and small sector angles.

Table 1 Convergence and comparison of frequency ($\Omega_1 = \omega R_2^2 \sqrt{\rho h / D}$) laminated (0/90) annular sector plates with clamped edges (R_1/R_2 = 0.5, h/R_2 = 0.2, E_1/E_2 = 40, α = 120°)

Modes	Reference results	Present DSC results-FSDT (N_s =11)			
	Pang *et al.* (2017)	N_x = 11	N_x = 15	N_x = 17	N_x = 19
1	5.175	5.1804	5.1804	5.1804	5.1804
2	5.694	5.7063	5.7063	5.7063	5.7063
3	6.619	6.6236	6.6236	6.6236	6.6236
4	7.809	7.8169	7.8169	7.8169	7.8169
5	9.150	9.1637	9.1637	9.1637	9.1637

Table 2 Comparison of frequency ($\Omega_1 = \omega R_2^2 \sqrt{\rho h / D}$) values of isotropic circular plates with simply supported edges

h/R_2	Reference results	Present DSC results-FSDT (N_s =11)			
	Khare and Mittal (2017)	N_s = 9	N_s = 11	N_s = 13	N_s = 15
0.1	4.8758	4.8749	4.8749	4.8749	4.8749
0.2	4.7606	4.7593	4.7593	4.7593	4.7593
0.3	4.5957	4.5881	4.5881	4.5881	4.5881
0.4	4.3975	4.3914	4.3912	4.3912	4.3912
0.5	4.1834	4.1768	4.1765	4.1765	4.1765

Table 3 Frequency values ($\Omega_1 = \omega R_1 \sqrt{\rho h / A_{11}}$) of laminated (0/90/0/90) S-C annular plate (h/R_1 = 0.1; R_1/R_2 = 1/3)

DSC				
Modes	Wang *et al*. (2016)	N = 11	N = 13	N = 15
1	0.32783	0.33924	0.33924	0.33924
2	0.32961	0.33068	0.33068	0.33068
3	0.34780	0.35496	0.35496	0.35496
4	0.40656	0.41136	0.41135	0.41135
5	0.51503	0.52479	0.52477	0.52477

HDQ				
Modes	Wang *et al*. (2016)	N = 11	N = 13	N = 15
1	0.32783	0.33715	0.33713	0.33713
2	0.32961	0.33008	0.33008	0.33008
3	0.34780	0.35199	0.35196	0.35196
4	0.40656	0.41086	0.41085	0.41085
5	0.51503	0.52301	0.52297	0.52297

The effects of boundary conditions and core lamina angles

Table 4 Frequency values $(\Omega_1 = \omega R_2^2\sqrt{\rho h/D})$ of (0/30/0) laminated circular plates (h/R_2 = 0.2) with clamped edges

Present DSC results				
h/R_2	N = 9	N = 11	N = 13	N = 15
0.1	8.1005	8.1003	8.1003	8.1003
0.2	7.1593	7.1593	7.1593	7.1593
0.3	6.1727	6.1724	6.1724	6.1724
0.4	5.3105	5.3102	5.3102	5.3102
0.5	4.6170	4.6167	4.6167	4.6167

Table 5 Convergence and comparison of frequency $(\Omega_1 = \omega R_2^2\sqrt{\rho/Eh^2})$ laminated (0/90/0/90) annular sector plates with clamped edges (R_1/R_2 = 0.5, E_1/E_2 = 15, α = 90°)

Modes	Present results (N_s = 11)				
	h/R_2	N_x = 9	N_x = 11	N_x = 13	N_x = 15
1	0.05	13.7123	13.7123	13.7123	13.7123
	0.1	9.3421	9.3421	9.3421	9.3421
	0.2	5.3684	5.3684	5.3684	5.3684
2	0.05	15.5729	15.5727	15.5727	15.5727
	0.1	10.9030	10.9028	10.9028	10.9028
	0.2	6.3455	6.3453	6.3453	6.3453
3	0.05	19.65039	19.6501	19.6501	19.6501
	0.1	13.6127	13.6124	13.6124	13.6124
	0.2	7.8919	7.8916	7.8916	7.8916
4	0.05	25.3490	25.3483	25.3483	25.3483
	0.1	17.0192	17.0181	17.0181	17.0181
	0.2	9.6808	9.6802	9.6802	9.6802
5	0.05	30.3021	30.3016	30.3016	30.3016
	0.1	18.7213	18.7205	18.7205	18.7205
	0.2	10.1966	10.1962	10.1959	10.1959

Table 6 Frequency $(\Omega_1 = \omega R_1\sqrt{\rho h/A_{11}})$ values of laminated (0/90) annular sector plates with clamped supported edges (E_1/E_2 = 2, R_1/R_2 = 1/2)

h/R	φ	Present results (N_x = 11)			
		N_x = 11	N_x = 13	N_x = 15	N_x = 17
0.1	90	6.5375	6.5375	6.5375	6.5375
	180	6.2348	6.2348	6.2348	6.2348
	270	6.1796	6.1796	6.1796	6.1796
0.2	90	4.5785	4.5785	4.5785	4.5785
	180	4.3519	4.3519	4.3519	4.3519
	27	4.3027	4.3027	4.3027	4.3027

Table 7 Frequency $(\Omega_1 = \omega R_1\sqrt{\rho h/A_{11}})$ laminated (0/90/0/90) circular plates with simply supported edges

h/R_2	Modes	Present results (N_x = 11)			
		N_x = 9	N_x = 11	N_x = 13	N_x = 15
0.01	1	5.6236	5.6236	5.6236	5.6236
	2	13.4408	13.4408	13.4408	13.4408
	3	24.3378	24.3375	24.3375	24.3375
	4	36.2813	36.2811	36.2811	36.2811
	5	38.1010	38.1003	38.1003	38.1003
0.1	1	5.2934	5.2931	5.2931	5.2931
	2	11.7445	11.7440	11.7440	11.7440
	3	18.6398	18.6394	18.6394	18.6394
	4	19.5450	19.5443	19.5443	19.5443
	5	26.0377	26.0372	26.0372	26.0372
0.2	1	4.5941	4.5938	4.5937	4.5938
	2	8.8176	8.8174	8.8174	8.8174
	3	9.6023	9.6019	9.6019	9.6019
	4	13.8670	13.8667	13.8667	13.8667
	5	14.8196	14.8192	14.8190	14.8190

Table 8 Frequency values $(\Omega_1 = \omega R_2^2\sqrt{\rho h/D})$ of (0/30/0) laminated circular plates (h/R_2 = 0.2)

Present DSC results				
	N = 11		N = 15	
Modes	Clamped	Simply supported	Clamped	Simply supported
1	7.1593	3.2705	7.1593	3.2705
2	13.0281	8.8806	13.0281	8.8806
3	18.9175	14.7314	18.9175	14.7314
4	22.0339	18.0132	22.0339	18.0132

Table 9 Frequency values $(\Omega_1 = \omega R_2^2\sqrt{\rho h/D})$ of laminated circular plates (h/R_2 = 0.3) with clamped edge

DSC				
Modes	0/0/0	0/30/0	0/60/0	0/90/0
1	6.5208	6.2016	5.3482	4.9340
2	10.9913	10.6314	9.5622	8.6591
3	15.0871	14.9028	13.9243	12.9313
4	17.5493	17.0219	15.0217	13.8004
5	19.4305	19.3178	18.3711	17.6112

HDQ				
Modes	0/0/0	0/30/0	0/60/0	0/90/0
1	6.5196	6.2002	5.3470	4.9327
2	10.9890	10.6304	9.5613	8.6579
3	15.0861	14.9011	13.9234	12.9301
4	17.5478	17.0213	15.0208	13.7990
5	19.4297	19.3167	18.3700	17.6104

Table 10 Frequency $(\Omega_1 = \omega R_2^2 \sqrt{\rho/Eh^2})$ laminated (0/90/0) plates (h/R_2 = 0.2) with clamped edge

R_1/R_2	Modes	Present results (N_x = 11)			
		N_x = 11	N_x = 1,	N_x = 15	N_x = 17
0	1	6.8843	6.8843	6.8843	6.8843
	2	10.5567	10.5567	10.5567	10.5567
	3	14.7804	14.7804	14.7804	14.7804
	4	17.1025	17.1025	17.1025	17.1023
	5	19.1138	19.1138	19.1138	19.1138
0.5	1	5.1627	5.1627	5.1627	5.1627
	2	5.4139	5.4139	5.4139	5.4139
	3	5.9615	5.9615	5.9615	5.9615
	4	6.2034	6.2034	6.2034	6.2034
	5	6.5538	6.5538	6.5538	6.5537

Table 11 Frequency values$(\Omega_1 = \omega R_2^2 \sqrt{\rho h/D})$ of (0/90/0/90) laminated annular plates (h/R_2 = 0.05)

R_1/R_2	Present DSC results			
	N = 13		N = 15	
	Clamped	Simply supported	Clamped	Simply supported
0.2	25.0368	15.1692	25.0368	15.1692
0.4	22.0591	14.4067	22.0591	14.4067
0.8	8.4035	3.1039	8.4035	3.1039

have been analyzed and results given in Tables 8 and 9, respectively. It is seen that for all values of the modes, the frequency parameter decreases when increasing the core angle. The effect of radius ratio on frequency values of annular plates was carried out numerically and results depicted in Tables 10 and 11, respectively.

It is obtained from these tables that the radii ratios have also been significant effect on frequency values. Obviously, it is show that the frequency parameters of the plates tend to decrease as plate radius ratio is increased. Furthermore, this phenomenon is more pronounced for higher modes frequency. Finally, variaton of fundamental frequency with modulus ratio for laminated plates and sector angles have been analyzed and results plotted in Figs. 3 and 4. The results show that the frequency rises gradually with increase in ratio of modulus of Young. Also the frequency values decrease when the sector angles increased.

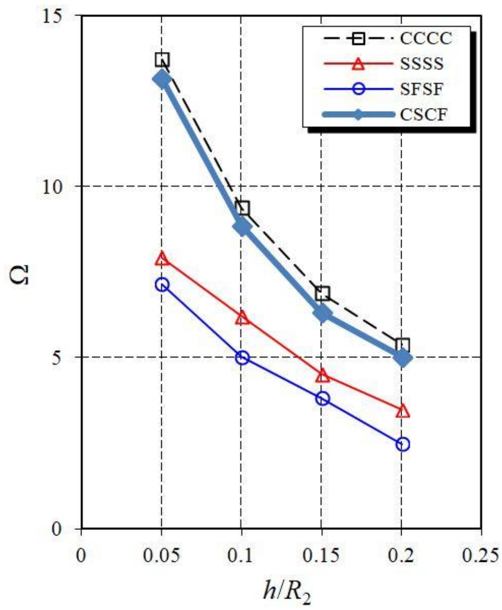

Fig. 2 Variation of fundamental frequency with thickness for different boundary conditions of laminated (0/90/0/90) annular sector plates (R_2/R_1 = 2; α = 90; E_1/E_2 = 15)

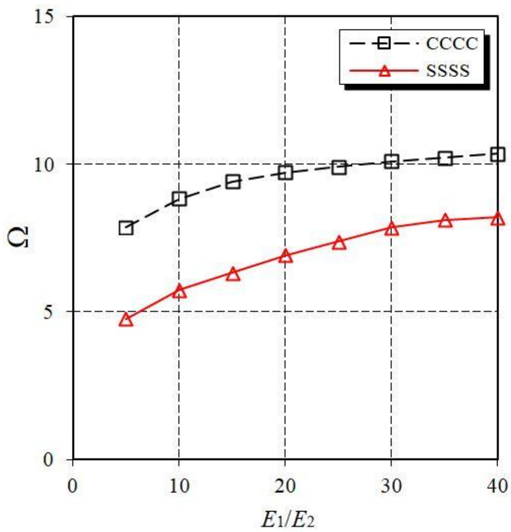

Fig. 3 Variation of fundamental frequency with modulus ratio for laminated (0/90/0/90) annular sector plates (R_2/R_1 = 2;α = 90; h/R_2 = 0.1)

6. Conclusions

In the present study, free vibration analyses of laminated circular and annular plates have been made via two-different numerical methods. Love's shell theory and first-order shear deformation theory (FSDT) have been used for modeling of plates. Different parameter effects on frequency values of laminated plates have been investigated in detail. The efficiency of the present two methods is validated by comparing the results with the previous published work. It is know that the accuracy and performance of the numerical methods depend on different parameters. In the method of differential quadrature the sampling of grid distribution and the grid numbers are the more significant than the other parameters for accuracy. As for the accuracy of the DSC method, there are different issue are important for accuracy and convergence. These are: kernel types, grid numbers, ghost numbers, regularized parameters etc. However, types of kernel and grid numbers are two important parameters on accuracy. Previous studies have shown that Shannon's delta kernel gives the best result. Also, DSC is more suitable for higher modes even

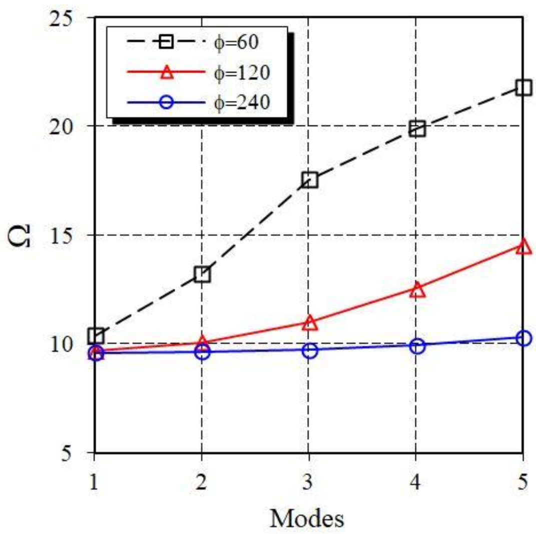

Fig. 4 Variation frequency with sector angles for laminated (0/90/90/0) annular sector plates ($R_2/R_1 = 2;\alpha = 90$; $h/R_2 = 0.1$; $E_1/E_2 = 15$) with CCCC edges

not investigated in this study. It is observed that the results obtained by HDQ method are at the same level of accuracy than those of previous technique DSC method. The novelty of the present study is based on the three remarks listed below:

- Both first-order shear deformation theory (FSDT) and the Love's shell theories have been used for modeling of annular, annular sector and circular plates.
- Governing equations of motion of annular and annular sector plates are directly obtained via conical shell equations.
- In order to solve the remaining governing partial differential equations related the plate vibration, two novels numerical methods have been performed and their performance are compared. It is shown that both methods have good convergence. Also, the method of DSC has shown a relatively fast approach with less grid points.
- *Effects of different material and geometric parameters on frequency values of annular and annular sector plates have been investigated.

Acknowledgments

The financial support of the Scientific Research Projects Unit of Akdeniz University is gratefully acknowledged.

References

Abdelaziz, H.H., Meziane, M.A.A., Bousahla, A.A., Tounsi, A., Mahmoud, S.R. and Alwabli, A.S. (2017), "An efficient hyperbolic shear deformation theory for bending, buckling and free vibration of FGM sandwich plates with various boundary conditions", *Steel Compos. Struct., Int. J.*, **25**(6), 693-704.

Aleksandrova, N.N. (2016), "Effect of thermal gradients on stress/strain distributions in a thin circular symmetric plate", *Struct. Eng. Mech., Int. J.*, **58**(4), 627-639.

Arefi, M, Mohammadi, M., Tabatabaeian, A., Dimitri, R. and Tornabene, F. (2018), "Two-dimensional thermo-elastic analysis of FG-CNTRC cylindrical pressure vessels", *Steel and Compos. Struct., Int. J.*, **27**(4), 525-536.

Thai, H.T. and Kim, S.E. (2013), "A simple quasi-3D sinusoidal shear deformation theory for functionally graded plates", *Compos. Struct.*, **99**, 172-180.

Bouchafa, A., Bouiadjra, M.B., Houari, M.S.A. and Tounsi, A. (2015), "Thermal stresses and deflections of functionally graded sandwich plates using a new refined hyperbolic shear deformation theory", *Steel Compos. Struct., Int. J.*, **18**(6), 1493-1515.

Bouderba, B., Houari, M.S.A., Tounsi, A. and Mahmoud, S.R. (2016), "Thermal stability of functionally graded sandwich plates using a simple shear deformation theory", *Struct. Eng. Mech., Int. J.*, **58**(3), 397-422.

Baltacıoglu, A.K., Akgöz, B. and Civalek, O. (2010), "Nonlinear static response of laminated composite plates by discrete singular convolution method", *Compos. Struct.*, **93**, 153-161.

Baltacıoğlu, A.K., Civalek, O., Akgöz, B. and Demir, F. (2011), "Large deflection analysis of laminated composite plates resting on nonlinear elastic foundations by the method of discrete singular convolution", *Int. J. Pres. Ves. Pip.*, **88**, 290-300.

Civalek, Ö. (1998), "Finite Element analysis of plates and shells", M.Sc. Dissertation; Fırat University, Elazığ, Turkey. [In Turkish]

Civalek, Ö. (2004), "Geometrically non-linear static and dynamic analysis of plates and shells resting on elastic foundation by the method of polynomial differential quadrature (PDQ)", Ph.D. Dissertation; Fırat University, Elazığ, Turkey. [In Turkish]

Civalek, O. (2006a), "The determination of frequencies of laminated conical shells via the discrete singular convolution method", *J. Mech. Mater. Struct.*, **1**(1), 163-182.

Civalek, O. (2006b), "Free vibration analysis of composite conical shells using the discrete singular convolution algorithm", *Steel Compos. Struct., Int. J.*, **6**(4), 353-366.

Civalek, O. (2008), "Analysis of thick rectangular plates with symmetric cross-ply laminates based on first-order shear deformation theory", *J. Compos. Mater.*, **42**, 2853-2867.

Civalek, O. (2013a), "Vibration analysis of laminated composite conical shells by the method of discrete singular convolution based on the shear deformation theory", *Compos. Part B: Eng.*, **45**(1), 1001-1009.

Civalek, O. (2013b), "Nonlinear dynamic response of laminated plates resting on nonlinear elastic foundations by the discrete singular convolution-differential quadrature coupled approaches", *Compos. Part B: Eng.*, **50**, 171-179.

Civalek, O. (2017), "Free vibration of carbon nanotubes reinforced (CNTR) and functionally graded shells and plates based on FSDT via discrete singular convolution method", *Compos. Part B: Eng.*, **111**, 45-59.

Civalek, O. and Acar, M.H. (2007), "Discrete singular convolution method for the analysis of Mindlin plates on elastic foundations", *Int. J. Pres. Ves. Pip.*, **84**, 527-535.

Civalek, O. and Akgöz, B. (2011), "Nonlinear vibration analysis of laminated plates resting on nonlinear two-parameters elastic foundations", *Steel Compos. Struct., Int. J.*, **11**(5), 403-421.

Civalek, O., Korkmaz, A. and Demir, Ç. (2010), "Discrete singular convolution approach for buckling analysis of rectangular Kirchhoff plates subjected to compressive loads on two opposite edges", *Adv. Eng. Softw.*, **41**, 557-560.

Civalek, O., Mercan, K. and Demir, C. (2016), "Vibration analysis of FG cylindrical shells with power-law index using discrete singular convolution technique", *Curved Layer. Struct.*, **3**, 82-90.

Demir, C., Mercan, K. and Civalek, O. (2016), "Determination of critical buckling loads of isotropic, FGM and laminated truncated conical panel", *Compos. Part B Eng.*, **94**, 1-10.

Duan, G., Wang, X. and Jin, C. (2014), "Free vibration analysis of circular thin plates with stepped thickness by the DSC element method", *Thin Wall. Struct.*, **85**, 25-33.

Fantuzzi, N. and Tornabene, F. (2014), "Strong formulation finite element method for arbitrarily shaped laminated plates- Part I. Theoretical analysis", *Adv. Aircr. Spacecr. Sci.*, **1**, 125-143.

Gürses, M., Civalek, Ö., Korkmaz, A. and Ersoy, H. (2009), "Free vibration analysis of symmetric laminated skew plates by discrete singular convolution technique based on first-order shear deformation theory", *Int. J. Numer. Methods Eng.*, **79**, 290-313.

Gürses, M., Akgöz, B. and Civalek, O. (2012), "Mathematical modeling of vibration problem of nano-sized annular sector plates using the nonlocal continuum theory via eight-node discrete singular convolution transformation", *Appl. Math. Comput.*, **219**, 3226-3240.

Hamzehkolaei, N.S., Malekzadeh, P. and Vaseghi, J. (2011), "Thermal effect on axisymmetric bending of functionally graded circular and annular plates using DQM", *Steel Compos. Struct., Int. J.*, **11**(4), 341-358.

Hou, Y., Wei, G.W. and Xiang, Y. (2005), "DSC-Ritz method for the free vibration analysis of Mindlin plates", *Int. J. Num. Meth. Eng.*, **62**, 262-288.

Jhung, M.J., Choi, Y.H. and Kim, H.J. (2005), "Natural vibration characteristics of a clamped circular plate in contact with fluid", *Struct. Eng. Mech., Int. J.*, **21**(2), 169-184.

Khare, S. and Mittal, N.D. (2016), "Three-dimensional free vibration analysis of thick laminated circular plates", *Int. J. Eng., Sci. Technol.*, **8**(2), 11-29.

Khare, S. and Mittal, N.D. (2017), "Free vibration of thick laminated circular and annular plates using three-dimensional finite element analysis", *AEJ - Alexandria Eng. J.*, **57**(3), 1217-1228.

Leissa, A.W. (1993), *Vibration of Shells*, Acoustical Society of America, Melville, NY, USA.

Malekzadeh, P. (2009), "Three-dimensional free vibration analysis of thick laminated annular sector plates using a hybrid method", *Compos. Struct.*, **90**, 428-437.

Mercan, K. and Civalek, O. (2016), "DSC method for buckling analysis of boron nitride nanotube (BNNT) surrounded by an elastic matrix", *Compos. Struct.*, **143**, 300-309.

Pang, F., Li, H., Miao, X. and Wang, X. (2017), "A modified Fourier solution for vibration analysis of moderately thick laminated annular sector plates with general boundary conditions, internal radial line and circumferential arc supports", *Curved Layer. Struct.*, **4**, 189-220.

Qatu, M. (2004), *Vibration of Laminated Shells and Plates*, Academic Press, UK.

Reddy, J.N. (2003), *Mechanics of Laminated Composite Plates And Shells: Theory and Analysis*, (2nd Edition), CRC Press, New York, NY, USA.

Saidi, A.R., Baferani, A.H. and Jomehzadeh, E. (2011), "Benchmark solution for free vibration of functionally graded moderately thick annular sector plates", *Acta Mech.*, **219**, 309-335.

Sharma, A., Sharda, H.B. and Nath, Y. (2005), "Stability and vibration of thick laminated composite sector plates", *J. Sound Vib.*, **287**, 1-23.

Shu, C. and Xue, H. (1997), "Explicit computations of weighting coefficients in the harmonic differential quadrature", *J. Sound Vib.*, **204**(3), 549-555.

Soedel, W. (2004), *Vibrations of Shells and Plates*, (3rd Edition), CRC Press, New York, NY, USA.

Striz, A.G., Wang, X. and Bert, C.W. (1995), "Harmonic differential quadrature method and applications to analysis of structural components", *Acta Mech.*, **111**, 85-94.

Su, Z., Jin, G. and Ye, T. (2014), "Three-dimensional vibration analysis of thick functionally graded conical, cylindrical shell and annular plate structures with arbitrary elastic restraints", *Compos. Struct.*, **118**, 432-447.

Su, Z., Jin, G. and Wang, X. (2015), "Free vibration analysis of laminated composite and functionally graded sector plates with general boundary conditions", *Compos. Struct.*, **132**, 720-736.

Tong, L. (1994), "Free vibration of laminated conical shells including transverse shear deformation", *Int. J. Solids Struct.*, **31**, 443-456.

Tornabene, F. and Fantuzzi, N. (2014), *Mechanics of Laminated Composite Doubly-curved Shell Structures, the Generalized Differential Quadrature Method and the Strong Formulation Finite Element Method*, Società Editrice Esculapio, Bologna, Italy.

Tornabene, F., Fantuzzi, N., Viola, E. and Ferreira, A.J.M. (2013), "Radial basis function method applied to doubly-curved laminated composite shells and panels with a General Higher-order Equivalent Single Layer formulation", *Compos. Part B: Eng.*, **55**, 642-659.

Tornabene, F., Fantuzzi, N. and Bacciocchi, M. (2014), "The local GDQ method applied to general higher-order theories of doubly-curved laminated composite shells and panels: the free vibration analysis", *Compos. Struct.*, **116**, 637-660.

Tornabene, F., Fantuzzi, N., Bacciocchi, M. and Viola, E. (2016), "Effect of agglomeration on the natural frequencies of functionally graded carbon nanotube-reinforced laminated composite doubly-curved shells", *Compos. Part B: Eng.*, **89**, 187-218.

Tahouneh, V. (2014), "Free vibration analysis of bidirectional functionally graded annular plates resting on elastic foundations using differential quadrature method", *Struct. Eng. Mech., Int. J.*, **52**, 663-686.

Wang, X., Wang, Y. and Xu, S. (2012), "DSC analysis of a simply supported anisotropic rectangular plate", *Compos. Struct.*, **94**, 2576-2584.

Wang, Q., Shi, D., Liang, Q. and Ahad, F. (2016a), "An improved Fourier series solution for the dynamic analysis of laminated composite annular, circular, and sector plate with general boundary conditions", *J. Compos. Mater.*, **50**(30), 4199-4233.

Wang, Q., Shi, D., Liang, Q. and e Ahad, F. (2016b), "A unified solution for free in-plane vibration of orthotropic circular, annular and sector plates with general boundary conditions", *Appl. Math. Model.*, **40**(21), 9228-9253.

Wei, G.W. (2001a), "Vibration analysis by discrete singular convolution", *J. Sound Vib.*, **244**, 535-553.

Wei, G.W. (2001b), "Discrete singular convolution for beam analysis", *Eng. Struct.*, **23**, 1045-1053.

Wei, G.W., Zhao, Y.B. and Xiang, Y. (2001), "The determination of natural frequencies of rectangular plates with mixed boundary conditions by discrete singular convolution" *Int. J. Mech. Sci.*, **43**, 1731-1746.

Wei, G.W., Zhao, Y.B. and Xiang, Y. (2002a), "A novel approach for the analysis of high-frequency vibrations", *J. Sound Vib.*, **257**, 207-246.

Wei, G.W., Zhao, Y.B. and Xiang, Y. (2002b), "Discrete singular convolution and its application to the analysis of plates with internal supports. Part 1: Theory and algorithm", *Int. J. Num. Meth. Eng.*, **55**, 913-946.

Wu, C.P. and Yu, L.T. (2016), "A state space meshless method for the 3D analysis of FGM axisymmetric circular plates", *Steel Compos. Struct., Int. J.*, **22**(1), 161-182.

Wu, C.P. and Yu, L.T. (2018), "Quasi-3D static analysis of two-directional functionally graded circular plates", *Steel Compos. Struct., Int. J.*, **27**(6), 789-801.

Yousefzadeh, S., Jafari, A.A., Mohammadzadeh, A. and Najafi, M.

(2018), "Dynamic response of functionally graded annular/circular plate in contact with bounded fluid under harmonic load", *Struct*. *Eng. Mech*., *Int. J*., **65**, 523-533.

CC

Appendix A

The related differential operators in above equations can be defined as

$$L_{11} = A_{11} \cdot U_{,xx} + \frac{A_{11}}{R(x)} \cdot \sin\alpha \cdot U_{,x} - \frac{A_{22}}{R^2(x)} \cdot U \cdot \sin^2\alpha + \frac{A_{33}}{R^2(x)} \cdot U_{,ss}$$

$$L_{12} = \frac{(A_{12} + A_{33})}{R(x)} \cdot \sin\alpha \cdot V_{,xs} - \frac{(A_{22} + A_{33})}{R^2(x)} \cdot \sin\alpha \cdot V_{,s}$$

$$L_{13} = \frac{A_{12}}{R(x)} \cos\alpha \cdot W_{,x} - \frac{A_{22}}{R^2(x)} \cdot W \cdot \sin\alpha \cdot \cos\alpha$$

$$L_{14} = B_{11} \cdot \Phi_{x,xx} + \frac{B_{11}}{R(x)} \cdot \sin\alpha \cdot \Phi_{x,x} - \frac{B_{22}}{R^2(x)} \cdot \Phi_{x} \cdot \sin^2\alpha + \frac{B_{33}}{R^2(x)} \cdot \Phi_{x,ss}$$

$$L_{15} = \frac{(B_{12} + B_{33})}{R(x)} \cdot \Phi_{s,xs} - \frac{(B_{22} + B_{33})}{R^2(x)} \cdot \sin\alpha \cdot \Phi_{s,s}$$

$$L_{21} = \frac{(A_{12} + A_{33})}{R(x)} \cdot U_{,xs} + \frac{(A_{22} + A_{33})}{R^2(x)} \cdot \sin\alpha \cdot U_{,s}$$

$$L_{22} = A_{33} \cdot V_{,xx} + A_{33} \frac{\sin\alpha}{R(x)} \cdot V_{,x}$$

$$- \frac{A_{33}}{R^2(x)} \cdot V \cdot \sin^2\alpha + \frac{A_{22}}{R^2(x)} \cdot V_{,ss} - \frac{A_{44}}{R^2(x)} \cdot V \cdot \cos^2\alpha$$

$$L_{23} = \frac{(A_{22} + A_{44})}{R^2(x)} \cdot \cos\alpha \cdot W_{,s}$$

$$L_{24} = \frac{(B_{12} + B_{33})}{R(x)} \cdot \Psi_{x,xs} + \frac{(B_{22} + B_{33})}{R^2(x)} \cdot \sin\alpha \cdot \Psi_{x,s}$$

$$L_{25} = B_{33} \cdot \Psi_{s,xx} + B_{33} \cdot \frac{1}{R(x)} \cdot \sin\alpha \cdot \Psi_{s,x}$$

$$- B_{33} \cdot \frac{1}{R^2(x)} \cdot \Psi_{s} \cdot \sin^2\alpha + B_{22} \frac{1}{R^2(x)} \cdot \Psi_{s,ss} + A_{44} \cdot \frac{1}{R(x)} \cdot \Psi_{s} \cdot \cos\alpha$$

$$L_{31} = -A_{12} \frac{1}{R(x)} \cdot \cos\alpha \cdot U_{,x} - A_{22} \cdot \frac{1}{R^2(x)} \cdot U \cdot \sin\alpha \cdot \cos\alpha$$

$$L_{32} = -\frac{(A_{22} + A_{44})}{R^2(x)} \cdot \cos\alpha \cdot V_{,s} \tag{A1}$$

$$L_{33} = A_{55} \cdot W_{,xx} + A_{55} \frac{1}{R(x)} \cdot \sin\alpha \cdot W_{,s}$$

$$+ A_{44} \cdot \frac{1}{R^2(x)} \cdot W_{,ss} - A_{22} \cdot \frac{1}{R^2(x)} \cdot W \cdot \cos^2\alpha$$

$$L_{34} = A_{55} \cdot \Psi_{x,x} - B_{12} \cdot \frac{1}{R(x)} \cdot \cos\alpha \cdot \Psi_{x,x}$$

$$+ A_{55} \cdot \frac{1}{R(x)} \cdot \Psi_{x} \cdot \sin\alpha - B_{22} \cdot \frac{1}{R^2(x)} \cdot \Psi_{x} \cdot \sin\alpha \cdot \cos\alpha$$

$$L_{35} = A_{44} \cdot \frac{1}{R(x)} \cdot \Psi_{s,s} - B_{22} \cdot \frac{1}{R^2(x)} \cdot \cos\alpha \cdot \Psi_{s,s}$$

$$L_{41} = B_{11} \cdot U_{,xx} + \frac{B_{11}}{R(x)} \cdot \sin\alpha \cdot U_{,x} - \frac{B_{22}}{R^2(x)} \cdot U \cdot \sin^2\alpha + \frac{B_{33}}{R^2(x)} \cdot U_{ss}$$

$$L_{42} = \frac{(B_{12} + B_{33})}{R(x)} \cdot V_{,xs} - \frac{(B_{22} + B_{33})}{R^2(x)} \cdot \sin\alpha \cdot V_{,s}$$

$$L_{43} = -A_{55} \cdot W_{,x} + B_{12} \cdot \frac{\cos\alpha}{R(x)} \cdot W_{,x} - \frac{B_{22}}{R^2(x)} \cdot W \cdot \sin\alpha \cdot \cos\alpha$$

$$L_{44} = D_{11} \cdot \Psi_{x,xx} + D_{11} \cdot \frac{\sin\alpha}{R(x)} \cdot \Psi_{x,x} - \frac{D_{22}}{R^2(x)} \cdot \Psi_{x} \cdot \sin^2\alpha$$

$$+ \frac{D_{33}}{R^2(x)} \cdot \Psi_{x,ss} - A_{55} \cdot \Psi_{x}$$

$$L_{45} = \frac{(D_{12} + D_{33})}{R(x)} \cdot \Psi_{s,xs} - \frac{(D_{22} + D_{33})}{R^2(x)} \cdot \Psi_{s,s} \cdot \sin\alpha$$

$$L_{51} = \frac{(B_{12} + B_{33})}{R(x)} \cdot U_{,xs} + \frac{(B_{22} + B_{33})}{R^2(x)} \cdot U_{,s} \cdot \sin\alpha$$

$$L_{52} = B_{33} \cdot V_{,xx} + B_{33} \frac{\sin\alpha}{R(x)} \cdot V_{,x}$$

$$
\begin{aligned}
&-B_{33}\cdot\frac{\sin^2\alpha}{R^2(x)}\cdot V+\frac{B_{22}}{R^2(x)}\cdot V_{,ss}+\frac{A_{44}}{R(x)}\cdot V\cdot\cos\alpha\\
&L_{53}=-\frac{A_{44}}{R(x)}\cdot W_{,s}+\frac{B_{22}}{R^2(x)}\cdot\cos\alpha\cdot W_{,s}\\
&L_{54}=\frac{(D_{12}+D_{33})}{R(x)}\cdot\Psi_{x,xs}+\frac{(D_{22}+D_{33})}{R^2(x)}\cdot\sin\alpha\cdot\Psi_{x,s}\\
&L_{55}=D_{33}\cdot\Psi_{s,xs}+D_{33}\cdot\frac{\sin\alpha}{R(x)}\cdot\Psi_{s}-\frac{D_{33}}{R^2(x)}\cdot\Psi_{s,x}\cdot\sin^2\alpha\\
&+\frac{D_{22}}{R^2(x)}\cdot\Psi_{s,ss}-A_{44}\cdot\Psi_{s}
\end{aligned}
\tag{A1}
$$

Appendix B

$$
\begin{aligned}
&G_{111}=-A_{22}\frac{\sin^2\alpha}{R^2(x)}-A_{66}\frac{n^2}{R^2(x)}\\
&G_{112}=A_{11}\frac{\sin\alpha}{R(x)}\\
&G_{113}=A_{11}\\
&G_{121}=-\frac{(A_{22}+A_{66})}{R^2(x)}n\sin\alpha-\frac{(B_{12}+B_{22}+2B_{66})}{R^3(x)}n\sin\alpha\cos\alpha\\
&G_{122}=\frac{(A_{12}+A_{66})}{R(x)}n+\frac{(B_{12}+2B_{66})}{R^2(x)}n\cos\alpha\\
&G_{131}=-A_{22}\frac{\sin\alpha\cos\alpha}{R^2(x)}-\frac{(B_{12}+B_{22}+2B_{66})n^2\sin\alpha}{R^3(x)}\\
&G_{132}=A_{12}\frac{\cos\alpha}{R(x)}+B_{22}\frac{\sin^2\alpha}{R^2(x)}+\frac{(B_{12}+2B_{66})n^2}{R^2(x)}\\
&G_{133}=-B_{11}\frac{\sin\alpha}{R(x)}\\
&G_{134}=-B_{11}\\
&G_{211}=-\frac{(A_{22}+A_{66})}{R^2(x)}n\sin\alpha-\frac{(B_{22}-B_{66})}{R^3(x)}n\sin\alpha\cos\alpha\\
&G_{212}=-\frac{n\cos\alpha}{R^2(x)}(B_{12}+B_{66})-\frac{n}{R(x)}(A_{12}+A_{66})\\
&G_{221}=-\frac{(A_{22}n^2+A_{66}\sin^2\alpha)}{R^2(x)}-\frac{(2B_{22}n^2-B_{66}\sin^2\alpha)}{R^3(x)}\cos\alpha\\
&-\frac{(D_{22}n^2-4D_{66}\sin^2\alpha)\cos^2\alpha}{R^4(x)}\\
&G_{222}=\frac{A_{66}\sin\alpha}{R(x)}-\frac{B_{66}\sin\alpha\cos\alpha}{R^2(x)}-\frac{4D_{66}\sin\alpha\cos^2\alpha}{R^3(x)}\\
&G_{223}=A_{66}+\frac{3B_{66}\cos\alpha}{R(x)}+\frac{2D_{66}\cos^2\alpha}{R^2(x)}\\
&G_{231}=-\frac{A_{22}n\cos\alpha}{R^2(x)}-\frac{B_{22}n(\cos^2\alpha+n^2)}{R^3(x)}-\frac{(D_{22}n^2-4D_{66}\sin^2\alpha)n\cos\alpha}{R^4(x)}\\
&G_{232}=\frac{B_{22}n\sin\alpha}{R^2(x)}+\frac{(D_{22}-4D_{66})n\cos\alpha\sin\alpha}{R^3(x)}\\
&G_{311}=-\frac{A_{22}\cos\alpha\sin\alpha}{R^2(x)}+\frac{(-B_{22}n^2+2B_{66}n^2+B_{22}\sin^2\alpha)\sin\alpha}{R^3(x)}\\
&G_{312}=-\frac{A_{12}\cos\alpha}{R(x)}-\frac{(-B_{12}n^2+2B_{66}n^2+B_{22}\sin^2\alpha)}{R^2(x)}\\
&G_{313}=\frac{2B_{11}\sin\alpha}{R(x)}\\
&G_{314}=B_{11}
\end{aligned}
\tag{B1}
$$

$$
\begin{aligned}
&G_{321}=-\frac{(A_{22}n\cos\alpha)}{R^2(x)}\\
&+\frac{(-D_{22}n^2+2D_{12}\sin^2\alpha+2D_{22}\sin^2\alpha+8D_{66}\sin^2\alpha)n\cos\alpha}{R^4(x)}\\
&+\frac{(-B_{22}n^2-B_{22}\cos^2\alpha+B_{22}\sin^2\alpha+2B_{66}\sin^2\alpha)n}{R^3(x)}\\
&G_{322}=\frac{(-D_{22}+2D_{12}+8D_{66})n\cos\alpha\sin\alpha}{R^3(x)}-\frac{(-B_{22}+2B_{66})n\sin\alpha}{R^2(x)}\\
&G_{323}=\frac{(B_{12}+2B_{66})n}{R(x)}+\frac{(D_{12}+4D_{66})n\cos\alpha}{R^2(x)}\\
&G_{331}=-\frac{A_{22}\cos^2\alpha}{R^2(x)}+\frac{(-2n^2+\sin^2\alpha)B_{22}\cos\alpha}{R^3(x)}\\
&+\frac{(-D_{22}n^2+2D_{12}\sin^2\alpha+2D_{22}\sin^2\alpha+8D_{66}\sin^2\alpha)n^2}{R^4(x)}\\
&G_{332}=-\frac{(D_{22}\sin^2\alpha+2D_{12}n^2+8D_{66}n^2)\sin\alpha}{R^3(x)}\\
&G_{333}=\frac{2B_{12}\cos\alpha}{R(x)}+\frac{2D_{12}n^2+4D_{66}n^2+D_{22}\sin^2\alpha}{R^2(x)}\\
&G_{334}=-\frac{2D_{11}}{R(x)}\sin\alpha\\
&G_{335}=-D_{11}
\end{aligned}
\tag{B1}
$$